Journal of Natural Medicines (2023) 77:403–411
https://doi.org/10.1007/s11418-023-01681-2

NOTE

Eumitrins I–K: three new xanthone dimers from the lichen *Usnea baileyi*

Van-Kieu Nguyen[1,2] · Phan-Si-Nguyen Dong[1,2] · Hoai-Vu Nguyen-Si[1,2] · Ek Sangvichien[3] · Thanh-Nha Tran[4] · Le-Thuy-Thuy-Trang Hoang[4] · Minh-Trung Dao[4] · Hai-Nguyen[1,2] · Hoang-Vinh-Truong Phan[1,2] · Hioki Yusuke[5] · Tohru Mitsunaga[6] · Warinthorn Chavasiri[7]

Received: 19 October 2022 / Accepted: 11 January 2023 / Published online: 7 February 2023

Abstract

In the continuing discovery and structure elucidation of natural xanthone dimers, which are still rarely reported in absolute configuration, three new xanthone dimers, eumitrins I–K (**1**–**3**) were isolated from the lichen *Usnea baileyi*, a rich source of natural xanthone dimers. Their structures were elucidated unambiguously by spectroscopic analyses, including high-resolution electrospray ionization mass spectrometry (HRESIMS), 1D and 2D nuclear magnetic resonance spectroscopy (1D and 2D NMR). The absolute configuration of all three compounds was established through DP4 probability and ECD calculation. All compounds revealed weak activity for their enzymatic inhibition against α-glucosidase and tyrosinase, as well as antibacterial activity.

Graphical abstract

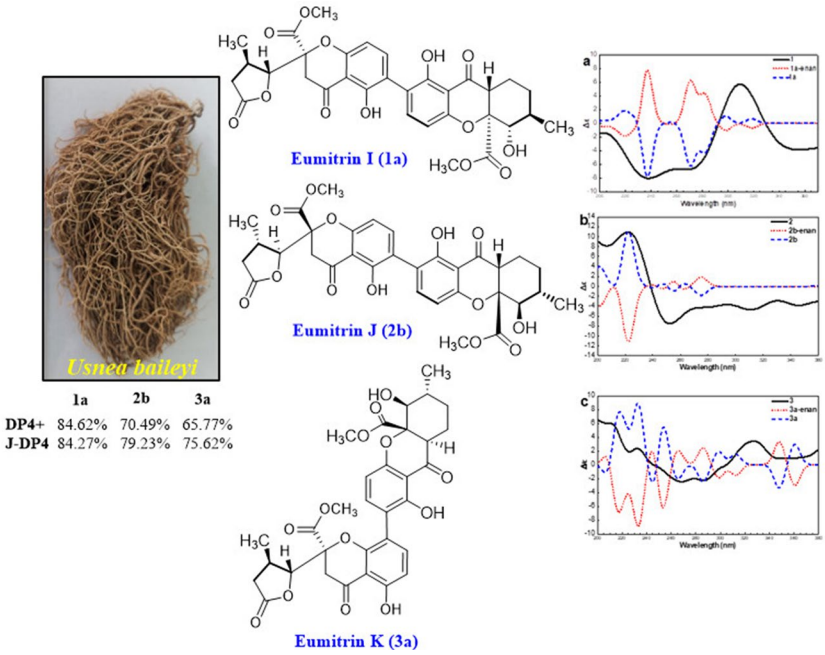

Keywords Lichen · *Usnea baileyi* · Dimeric xanthone · α-Glucosidase · Enzyme inhibitory · Antibacterial

Extended author information available on the last page of the article

Introduction

The xanthone dimers comprising a hexahydroxanthone monomer and a chromanone lactone are complicated structural compounds widely distributed in fungi and lichens [1–5]. They are reported to occur as mycotoxins with toxic, fetotoxic/teratogenic, and mutagenic properties [6], as well as cytotoxic substances against cancer cells [7], and having α-glucosidase inhibition [8]. Although the absolute configurations for the foregoing heterodimers have been established directly by X-ray crystal diffraction analysis [7, 9–11] and indirectly by ECD calculations [12, 13], the determination of the relative and absolute configurations of their structures is a challenge due to the numerous chirality centers with axial chirality elements in some cases. Therefore, the assignment of the absolute configurations in many cases of xanthone dimers is incomplete. Currently, many reports have revealed the isolation and structural elucidation of the xanthone dimers from the lichen genus *Usnea* sp. such as those from *U. aciculifera* [7, 9] or *U. baileyi* [8, 12, 14]. However, many dimeric xanthones, such as eumitrin A3, B2 from *U. baileyi* [15] and eumitrin U, X, or Y from other lichen sources [16–18] were described without structural determination, leading to interest in the isolation and structural elucidation of these compounds. During our phytochemical investigation of *U. baileyi*, numerous xanthone dimers were reported such as bailexanthone [14] and eumitrins C–H [8, 12]. In the continuous study on new xanthone dimers and their absolute configurations from *U. baileyi*, our current study reports the isolation, structure elucidation, and evaluation of enzyme inhibitory activity against α-glucosidase and tyrosinase, and antibacterial activity of three new xanthone dimers: eumitrins I–K (**1**–**3**).

Results and discussion

Continuing chromatographic fractionation of the acetone extract of *U. baileyi* led to the purification of three new compounds that showed the same molecular formulas $C_{32}H_{32}O_{13}$ from HRESIMS namely eumitrins I–K (**1**–**3**). In addition, their UV–vis (Fig. S1) and IR (Fig. S2) spectra were also quite similar, indicating that they shared related skeletons. The doubled resonances in the 1D NMR (Table 1), particularly in the ^{13}C NMR spectra of **1**–**3**, suggested that they are xanthone heterodimers further supported by the comparison of 1D NMR of **1**–**3** to those of bailexanthone and eumitrin series isolated in the same bio-source [8, 12, 14] (Fig. 1).

Compound **1** was isolated as a light yellow gum. The occurrence of a hexahydroxanthone moiety of the first subunit was determined by the near-identical 1D NMR data of **1** to those of bailexanthone [14], eumitrin C [12], and eumitrin F–G [8], evidenced by the HMBC correlation from both methine H-8a (δ_H 3.00) and oxymethine H-5 (δ_H 3.73) to C-10 (δ_C 87.5), from oxymethine H-5 and methyl H_3-11 (δ_H 1.12) to C-7 (δ_C 31.2). Moreover, a methyl ester group allocated at oxygenated carbon C-10 was identified by the HMBC correlation from both the methine protons H-5, H-8a and methoxy proton H_3-13 (δ_H 3.68) to C-12 (δ_C 169.2). A second spin system in this monomer is a phenyl ring moiety supported by HMBC correlations from the aromatic protons H-3 and H-4 at δ_H 7.48 and 6.62, respectively, to C-4a (Fig. 2). In addition as the two Hα at H_2-8a′ can cause hyperconjugation to C-9′ as an electron-donating effect which contributes more electrons to C-9′ than those of a single Hα at H-8a to C-9, further supported by the ^{13}C NMR data of C-9 and C-9′ as 197.4 and 194.2, respectively. Thus, the chemical shift of 1-OH and 1′-OH was identified at δ_H 11.91 and 11.89, respectively, further demonstrated by HMBC correlations from the phenolic proton at δ_H 11.91 to C-1 (δ_C 159.1), C-2 (δ_C 118.1) and C-9a (δ_C 107.4). Due to C-2 being a quaternary carbon, it can be deemed that this specific site is linked to the other part of the compound.

Furthermore, the occurrence of 2,2-disubstituted chromanone monomeric unit was assigned by the 2D NMR correlations and the similar 1D NMR data to those of eumitrin D [12], versixanthones A–D [10]. The connection between the γ-butyrolactone moiety and the chromanone monomeric unit was identified by the HMBC cross-peak between H-5′ (δ_H 4.81) and C-12′ (δ_C 169.2).

The planar structure of **1** was formed by connecting the two monomeric units through the linkage of hexahydroxanthone C-2 and chromanone C-2′, supported by the HMBC correlations of H-3′ (δ_H 7.53) with C-2, H-3 (δ_H 7.48) with C-2′ (δ_C 117.4), and 1′-OH (δ_H 11.89) with C-1′, C-1′ and C-9a′ (δ_C 107.4) (Fig. 2).

The relative configuration of **1** was readily recognized to be the same as that of eumitrin G [8], blennolides [19], blennolides I and J [20] based on the coupling constant ($^3J_{H\text{-}5,\,H\text{-}6}$ = 10.5 Hz), the NOESY correlation between H-5, H-8a and H_3-11 (Fig. 3), and the chemical shifts similarities (Table 1). Moreover, the *cis* configuration of H-5′ and H_3-11′ in the γ-butyrolactone moiety was identified by the NOESY correlation between H-5′ and H_3-11′.

Similar to **1**, compounds **2** and **3** were also built from hexahydroxanthone and chromanone monomers, except for the different configuration on hexahydroxanthone (for **2**) or linkage pattern (for **3**). As for compound **2**, the coupling constant ($^3J_{H\text{-}5,\,H\text{-}6}$ = 7.2 Hz), the NOESY correlation between H-5 and H_3-11, H-8a and H-6 (Fig. 3), and the chemical shift similarities (Table 1) indicated the relative configuration of the hexahydroxanthone monomer to be the same as that of eumitrin F [8]. For **3**, the 4-2′ linkage of two monomers was

Table 1 ^{1}H and ^{13}C NMR data for **1–3** in $CDCl_3$ (δ ppm)

No.	**1***		**2****		**3***	
	δ_H (*J*, Hz)	δ_C	δ_H (*J*, Hz)	δ_C	δ_H (*J*, Hz)	δ_C
1		159.1		159.5		159.1
2		118.1		118.1		117.2
3	7.48 (1H, *d*, 8.5)	140.3	7.48 (1H, *d*, 9.0)	141.0	7.65 (1H, *d*, 9.0)	140.7
4	6.62 (1H, *d*, 8.5)	107.4	6.63 (1H, *d*, 8.4)	107.7	6.64 (1H, *d*, 7.0)	108.1
4a		158.5		158.5		158.7
5	3.73 (1H, *d*, 10.5)	80.3	3.88 (1H, *d*, 7.2)	74.1	3.77 (1H, *d*, 11.0)	82.5
6	1.82 (1H, *m*)	34.3	1.81 (1H, *m*)	27.3	1.86 (1H, *m*)	34.0
7	1.95 (1H, *m*); 1.19 (1H, *m*)	31.2	2.05 (1H, *m*); 1.29 (1H, *m*)	33.6	1.95 (1H, *m*); 1.28 (1H, *m*)	31.2
8	2.20 (1H, *m*); 2.14 (1H, *m*)	20.4	2.26 (1H, *m*); 2.18 (1H, *m*)	21.5	2.19 (2H, *m*)	20.4
8a	3.00 (1H, *dd*, 11.5, 5.0)	51.2	3.41 (1H, *dd*, 7.2, 4.8)	46.4	3.05 (1H, *dd*, 11.0, 5.5)	51.2
9		197.4		198.7		197.7
9a		107.6		107.5		108.0
10		87.5		85.6		86.0
11	1.12 (3H, *d*, 6.5)	18.4	1.12 (3H, *d*, 7.2)	17.8	1.12 (3H, *d*, 6.5)	18.5
12		169.2		170.1		169.3
13	3.68 (3H, *s*)	53.0	3.77 (3H, *s*)	53.4	3.76 (3H, *s*)	53.0
1′		159.3		159.3		161.9
2′		117.4		117.5	6.64 (1H, *d*, 7.0)	110.5
3′	7.53 (1H, *d*, 8.5)	141.4	7.53 (1H, *d*, 8,4)	141.4	7.55 (1H, *d*, 8.5)	141.7
4′	6.62 (1H, *d*, 8.5)	107.4	6.58 (1H, *d*, 8.4)	107.6		115.5
4a'		159.0		157.4		158.7
5′	4.81 (1H, *d*, 6.5)	82.9	4.81 (1H, *d*, 7.2)	82.8	4.66 (1H, *d*, 7.5)	80.1
6′	2.96 (1H, *m*)	33.6	2.98 (1H, *m*)	36.1	2.88 (1H, *m*)	34.1
7′	2.70 (1H, *dd*, 17.0, 8.0); 2.48 (1H, *dd*, 17.0, 8.0)	36.9	2.71 (1H, *dd*, 17.4, 8.4) 2.48 (1H, *dd*, 17.4, 7.8)	36.9	2.28 (1H, *dd*, 17.0, 8.5) 2.00 (1H, *dd*, 17.0, 7.5)	35.6
8′		174.9		175.0		174.8
8a′	3.27 (1H, *d*, 17.5) 3.20 (1H, *d*, 17.0)	39.9	3.28 (1H, *d*, 17.4) 3.21 (1H, *d*, 17.4)	39.9	3.27 (1H, *d*, 17.5) 3.16 (1H, *d*, 17.5)	40.0
9′		194.2		194.2		194.1
9a′		107.4		106.8		107.5
10′		84.6		84.6		87.7
11′	1.33 (3H, *d*, 7.0)	15.0	1.34 (3H, *d*, 7.2)	15.0	1.23 (3H, *d*, 7.0)	14.8
12′		169.2		169.2		168.9
13′	3.77 (3H, *s*)	53.9	3.84 (3H, *s*)	53.9	3.69 (3H, *s*)	53.8
1-OH	11.91 (1H, *s*)		12.21 (1H, *s*)		11.79 (1H, *s*)	
1′-OH	11.89 (1H, *s*)		11.92 (1H, *s*)		11.62 (1H, *s*)	

*^{1}H (500 MHz) and ^{13}C (125 MHz) NMR

**^{1}H (600 MHz) and ^{13}C (150 MHz) NMR

recognized by HMBC correlations from H-3 to C-4′ and from H-3' to C-2 (Fig. 2).

Due to the NOESY correlation between H-5 and H_3-11, H-5′ and H_3-11′ (Fig. 3), along with the identical ^{13}C NMR data of enantiomers, the two diastereomeric candidates for each compound (**1a/1b**, **2a/2b**, and **3a/3b**) were proposed (Fig. 4), which would be determined via the DP4 parameter.

As shown in Table S1, the p_i values of **1a** are nearly equal while those of **1b** have a large difference. The three **1a** conformers have the highest p_i (**1a01**—9.434%, **1a02**—9.901%, and **1a03**—9.600%), and these values are only about 2% higher than the latter group. Besides, there are four **1b** conformers having the highest p_i (**1b01**—18.577%, **3b08**—12.144%, **1b09**—11.819%, and **1b12**—17.810%),

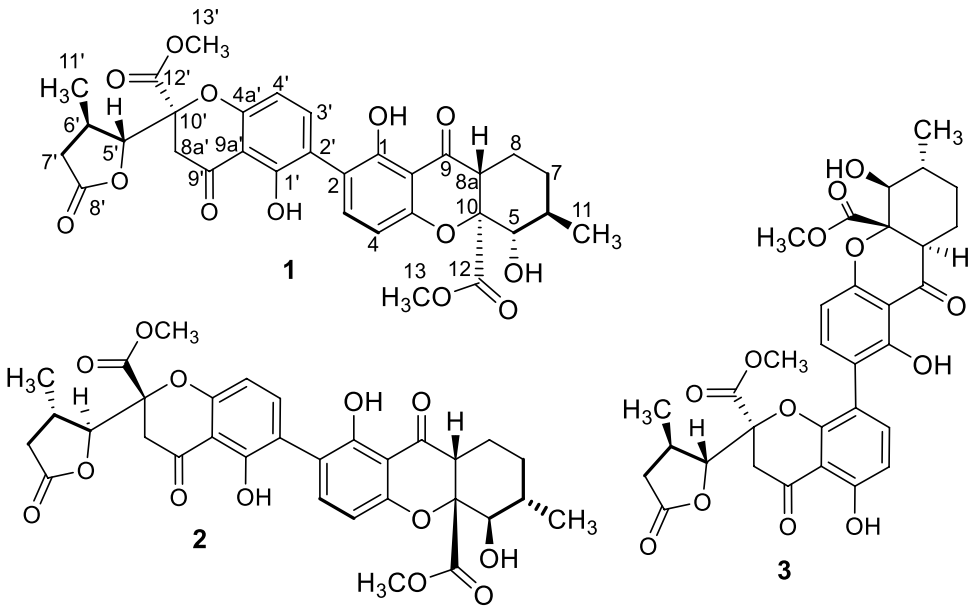

Fig. 1 Chemical structures of compounds **1**–**3**

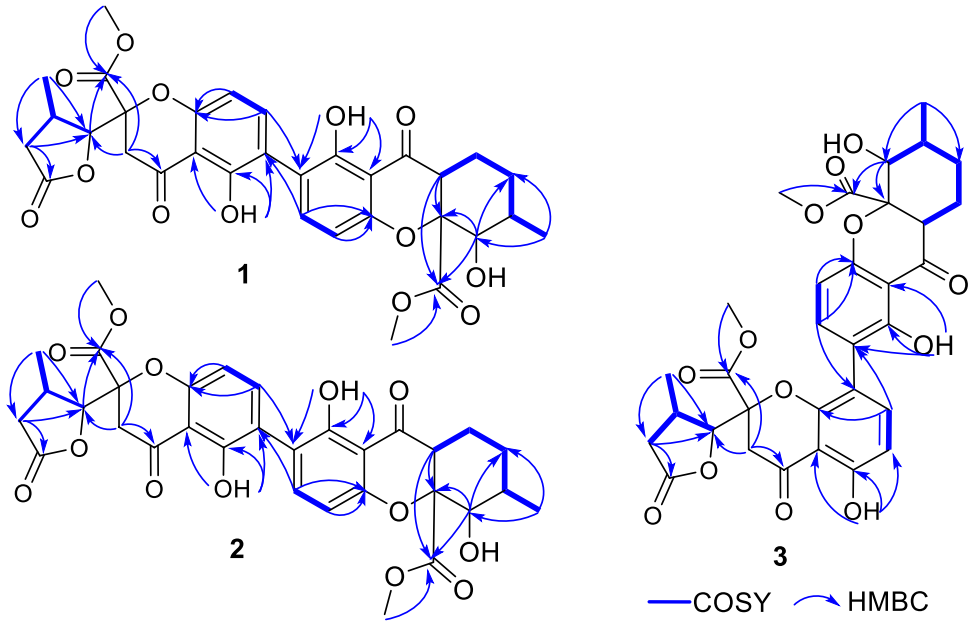

Fig. 2 Key ^{1}H–^{1}H COSY and HMBC correlations for **1**–**3**

these values are 10% higher than the latter group. The p_i of selected groups (**1a01**–**1a17** and **1b01**–**1b12**) accounted for over 90% of **1a** and **1b** total p_i, indicating that the selected groups are statistically representative of the substances. Furthermore, DP4 probabilities (DP4 + and J-DP4) of **1a** (ave.) are much higher than that of **1b** (ave.) (84.62% and 84.27% compared to 15.38% and 15.73%). These values suggest that **1a** structures give the most consistent simulation results compared to the experimental spectrum. In the same manner, as those of **1**, **2b** (with DP4+ and J-DP4 percentages as 70.49% and 79.23%, respectively, Table S2), and **3a** (with DP4+ and J-DP4 percentages as 65.77% and 75.62%, respectively, Table S3) would be the proper structure for **2** and **3**, respectively, that were further used for absolute configuration determination through ECD calculation (Fig. 5).

The DP4 peak assignment (by DP4+ and J-DP4 methods) showed that **1a**, **2b**, and **3a** represent **1**, **2**, and **3**, respectively with overwhelming probability values compared to

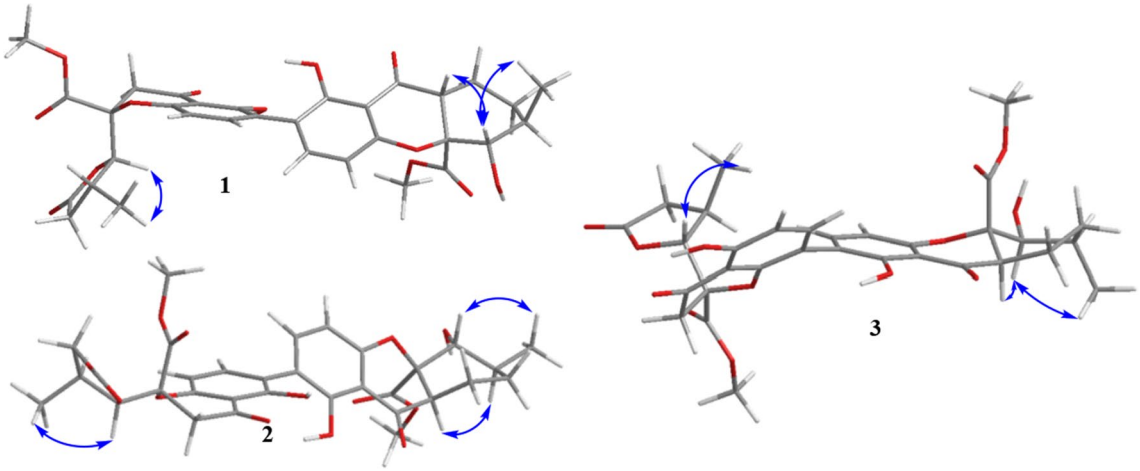

Fig. 3 Key NOESY correlations for **1**–**3**

the remaining conformers/structures. The experimental ECD spectra of **1**–**3** were compared with calculated ones.

The experimental spectrum was well matched with that of **1a**, **2b**, and **3a**. Thus, the absolute configuration of **1**–**3**, namely eumitrins I–K, were established as (5*S*,6*R*,8a*R*,10a*S*,5′*R*,6′*R*,10a′*S*)-1, (5*R*,6*S*,8a*R*,10a*R*,5′*S*,6′*S*,10a′*R*)-2, and (5*S*,6*R*,8a*R*,10aS,5′*R*,6′*R*,10a′*S*)-3, respectively.

In our previous report, eumitrins F–H revealed good activity on antimicrobial (eumitrins F–G) and enzyme inhibition against α-glucosidase [8]. In this study, compounds **1**–**3** were also evaluated for their antimicrobial activity and enzyme inhibition against tyrosinase and α-glucosidase (Table S4). Unfortunately, **1**–**3** revealed weak (compounds **1**, **3**) or no (compound **2**) antimicrobial activity (Table S4). As to enzyme inhibitory activities, only compound **1** showed a weak effect against tyrosinase (Table S4) with an IC_{50} value of 148.5 μM.

Experimental

General experiment procedures

Optical rotations were measured on a JASCO P-1010 polarimeter (JASCO, Easton, MD, USA). The UV measurements were done using a Hitachi U4100 instrument. The IR spectra were measured on Frontier FTIR/NIR spectrometers (Perkin Elmer, USA). The experimental ECD data were recorded on a JASCO J-815 spectropolarimeter. HRESIMS spectra were recorded on Bruker micrOTOF Q-II and MALDI-TOF-MS mass spectrometers. The 1D and 2D NMR spectra were acquired using a Bruker Advance spectrometer (500/125 MHz for ^{1}H and ^{13}C NMR, respectively) and a JEOL JNM-ECZR (600/150 MHz for ^{1}H and ^{13}C NMR, respectively).

The residual solvent signal ($CDCl_3$: $\delta_H = 7.26$, $\delta_C = 77.16$) was used to reference the chemical shifts. The column chromatography was performed using (0.040–0.063 mm, Himedia)-silica gel. TLC analysis was accomplished on silica gel 60 F_{254} or silica gel 60 RP-18 $F_{254}S$ plates (Merck), and a 10% H_2SO_4 solution was used to visualize the spots after heating.

Lichen material

The whole thalli of *Usnea baileyi* (Parmeliaceae) were collected and identified as stated in our previous report [8, 12, 14].

Extraction and isolation

In this work, we continue our study of further fractionation of the three fractions DCM2.2.1-3. The description for extraction and isolation was reported by Nguyen et al. [8, 12]. Compound **1** (2.4 mg) was obtained by further silica gel chromatographic column of DC2.2.2 (450.9 mg) eluted with *n*-hexane/CH_2Cl_2/MeOH (3:7:0.1) to yield compounds **1** (2.4 mg) while compounds **2** (4.6 mg) and **3** (5.2 mg) were isolated from DCM2.2.3 (385.7 mg) with *n*-hexane/CH_2Cl_2/EtOAc/MeOH (6:4:2:0.1).

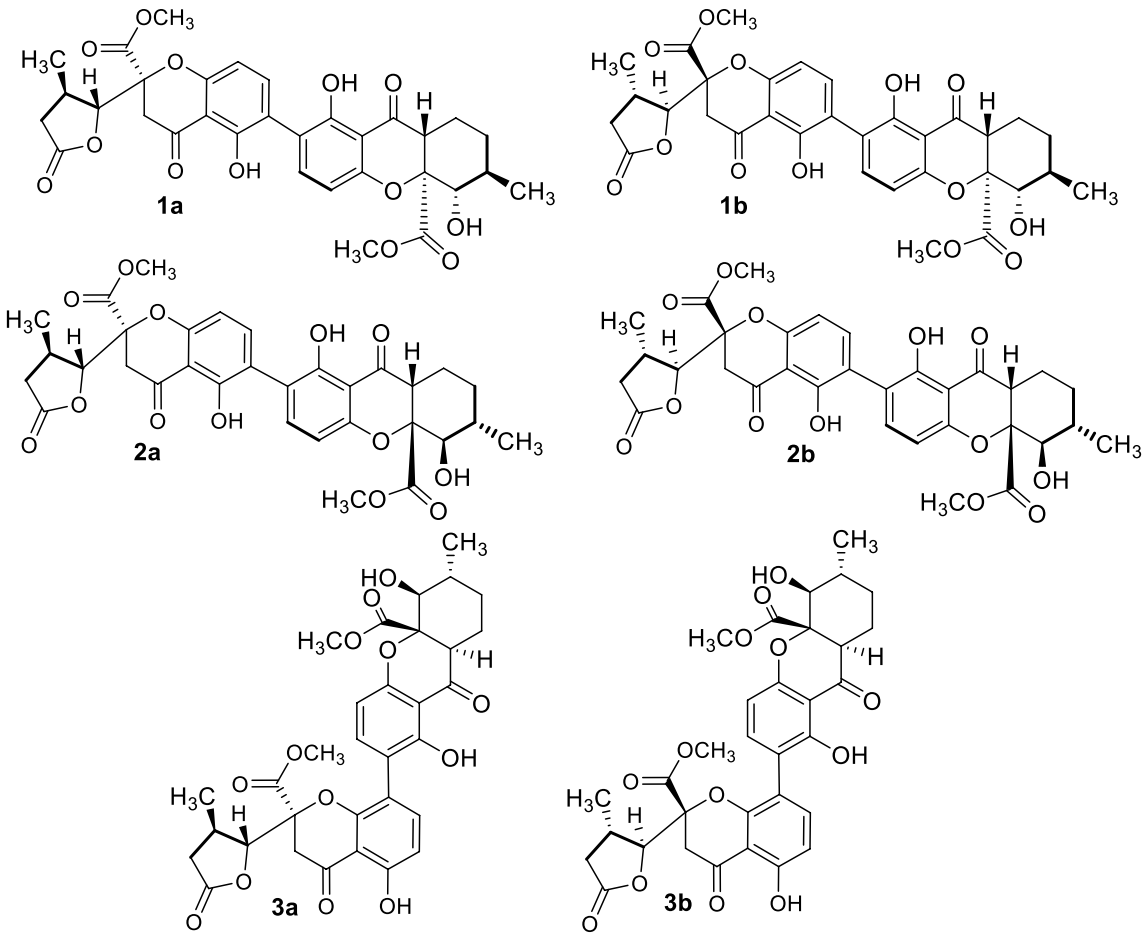

	1a	1b	2a	2b	3a	3b
DP4+	**84.62**%	15.38%	29.51%	**70.49**%	**65.77**%	34.23%
J-DP4	**84.27**%	15.73%	20.77%	**79.23**%	**75.62**%	24.38%

Fig. 4 Relative configuration for **1**–**3**: DP4+ , J-DP4 probabilities of the two candidate diastereomers

Compound 1 (Eumitrin I)

Yellow, amorphous solid; ^{1}H NMR ($CDCl_3$, 500 MHz) and ^{13}C NMR ($CDCl_3$, 125 MHz) see Table 1; IR (ATR) ν_{max} cm^{-1} 3513, 2933, 1739, 1625, 1430, 1363, 1199, 1053; UV λ_{max} (log ε) 207 (4.3), 266 (4.3), 367 (3.8) nm; $[\alpha]^{25}_{D}$—34.0 (c 0.02, MeOH); HRESIMS *m/z*: $[M+Na]^+$ 647.1740 for $C_{32}H_{32}O_{13}Na$ (calcd. 647.1741).

Compound 2 (Eumitrin J)

Yellow, amorphous solid; ^{1}H NMR ($CDCl_3$, 600 MHz) and ^{13}C NMR ($CDCl_3$, 150 MHz) see Table 1; IR (ATR) ν_{max} cm^{-1} 3506, 2933, 1737, 1628, 1437, 1363, 1198, 1049; UV λ_{max} (log ε) 236 (4.2), 267 (4.3), 373 (3.8) nm; $[\alpha]^{25}_{D}$—18.8 (c 0.02, MeOH); HRESIMS *m/z*: $[M+Na]^+$ 647.1766 for $C_{32}H_{32}O_{13}Na$ (calcd. 647.1741).

Compound 3 (Eumitrin K)

Yellow, amorphous solid; ^{1}H NMR ($CDCl_3$, 500 MHz) and ^{13}C NMR ($CDCl_3$, 125 MHz) see Table 1; IR (ATR) νmax cm^{-1} 3522, 2908, 1730, 1642, 1431, 1354, 1208, 1047; UV λ_{max} (log ε) 235 (4.3), 267 (4.4), 364 (3.8) nm; $[\alpha]^{25}_{D}$—258.8 (c 0.02, MeOH); HRESIMS *m/z*: $[M+Na]^+$ 647.1748 for $C_{32}H_{32}O_{13}Na$ (calcd. 647.1741).

Biological activities

The antimicrobial, tyrosinase, and α-glucosidase activity was performed according to our previous report [8].

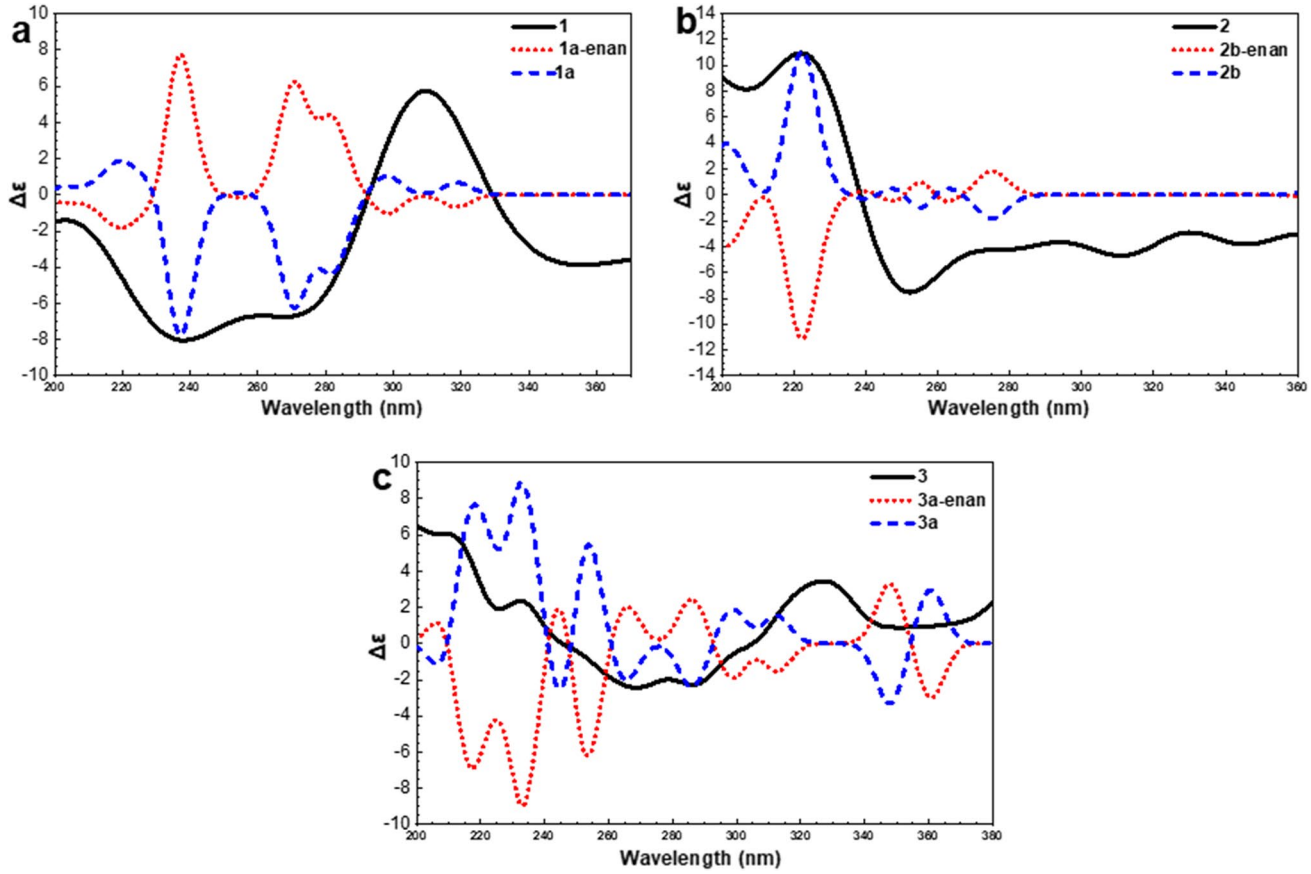

Fig. 5 Experimental ECD and calculated spectra of eumitrins I–K (**1**–**3**). **a** Experimental ECD spectrum of **1** and calculated ECD spectrum of (5*R*,6*S*,8a*S*,10a*R*,5′*S*,6′*S*,10a′*R*)-**1** (**1a-enan**). **b** Experimental ECD spectrum of **2** and calculated ECD spectrum of (5*S*,6*R*,8a*S*,10a*S*,5′*R*,6′*R*,10a′*S*)-**2** (**2a-enan**). **c** Experimental ECD spectrum of **3** and calculated ECD spectrum of (5*R*,6*S*,8a*S*,10a*R*,5′*S*,6′*S*,10a′*R*)-**3** (**3a-enan**)

Computational details

In this research, the Conformer–Rotamer Ensemble Sampling Tool (CREST) [21, 22] carried out conformer sampling for **1**–**3 (a/b)** structures (a total of six structures). These structures were embedded in (polarizable continuum model) $CHCl_3$ solvent. The CREST code utilized the GFN2-xTB algorithm to predict and arrange possible configurations (of the starting structures) in increasing total energy order. A 1.0 kcal/mol energy window (count from the lowest total energy configuration) was applied to eliminate configurations with total energies outside this range. Several configurations satisfying the above settings were extracted, including 23, 14, 10, 10, 10, and 8 conformers for **1a**, **1b**, **2a**, **2b**, **3a**, and **3b**, respectively. These (75) configurations were subjected to structure optimization and single-point energy calculation by ORCA code [23], employing the PBE0/def2-TZVP//PBE0/aug-cc-pVTZ level of theories. The single-point energy of each configuration was used to calculate the Boltzmann distribution (p_i) by the following equation.

$$p_i = \frac{\exp\left(-E_i/\mathrm{RT}\right)}{\sum_{j=1}^{\mathrm{all}} \exp\left(-E_j/\mathrm{RT}\right)} \quad (1)$$

In (Eq. 1), E_i and E_j are the conformer's total energies (in kcal/mol), and the RT value is 0.5925 kcal/mol at 298.15 K.

The ^{13}C NMR chemical shift calculation was executed on conformers with p_i above 3% (0.03) because the contribution of conformers with p_i lower than 3% is considered insignificant. Accordingly, there were 39 conformers selected, comprising 12, 10, 5, 5, 4, and 3 configurations corresponding to **1a**, **1b**, **2a**, **2b**, **3a**, and **3b**. The NMR chemical shift calculation was performed by ORCA code on optimized structures, using the PBE0/pcSseg-2 level of theory. To accurately determine a stereochemical structure from simulated NMR shifts, we need to compare the simulated peaks of configurations with the experimental spectrum, a procedure called peak assignment. The peak assignment process produces many errors that affect the results' accuracy. Smith and Goodman developed a probability method called DP4 [24] that could eliminate

systematic errors utilizing Bayes' theorem. This method has been widely adopted and developed into more advanced techniques such as DP4+ and J-DP4 [21, 25]. The DP4 family returns the results as a percentage (matching probability) of each configuration compared to the experimental spectrum. Accordingly, the highest DP4 value configuration will be the most suitable configuration for the initial structure. The authors applied DP4+ and J-DP4 methods in this research to verify the most feasible configuration for each initial structure. The selected configuration must have the highest matching probabilities in both DP4 processes and will be chosen as the sole representation of each given substance (**1**–**3**, **a/b**) to calculate simulated ECD spectra. The ECD calculation was performed by ORCA code on optimized structures (see ESI) and employed the PBE0/def2-TZVP//B3LYP/def2-TZVPP level of theories. The polarize basis-set (def2-TZVPP) was chosen because it can better represent the interaction of the orbitals with the stimulated wavelength in UV regions.

Conclusion

In this study, the continuing fractionation of DCM2.2.1-3 of CH_2Cl_2 extract from lichen *Usnea baileyi* led to the isolation of three new xanthone dimers namely eumitrins I–K (**1**–**3**). Their planar structures were elucidated based on the HRESIMS and NMR spectroscopic data. The absolute stereochemistry of **1**–**3** was determined by DP4 parameters and ECD calculation. All of the tested compounds revealed weak or inactive α-glucosidase, tyrosinase, and antimicrobial activity.

Supplementary Information The online version contains supplementary material available at https://doi.org/10.1007/s11418-023-01681-2.

Acknowledgements Nguyen V-K would like to thank N. Dangphui for the authentication of the lichen material. Thanks are also extended to the graduate school of Chulalongkorn University to provide 90th year anniversary scholarship.

Funding Chulalongkorn University to provide 90th year anniversary scholarship.

Data availability All data generated or analysed during this study are included in this published article (and its supplementary information files).

Declarations

Conflict of interest No potential conflict of interest was reported by the authors.

References

1. Masters KS, Bräse S (2012) Xanthones from fungi, lichens, and bacteria: the natural products and their synthesis. Chem Rev 112(7):3717–3776. https://doi.org/10.1021/cr100446h
2. Wezeman T, Bräse S, Masters K-S (2015) Xanthone dimers: a compound family which is both common and privileged. Nat Prod Rep 32(1):6–28. https://doi.org/10.1039/C4NP00050A
3. Le Pogam P, Boustie J (2016) Xanthones of lichen source: a 2016 update. Molecules 21(3):294–323. https://doi.org/10.3390/molecules21030294
4. Cai S, King JB, Du L, Powell DR, Cichewicz RH (2014) Bioactive sulfur-containing sulochrin dimers and other metabolites from an *Alternaria* sp. isolate from a Hawaiian soil sample. J Nat Prod 77(10):2280–2287. https://doi.org/10.1021/np5005449
5. Kikuchi H, Isobe M, Kurata S, Katou Y, Oshima Y (2012) New dimeric and monomeric chromanones, gonytolides D-G, isolated from the fungus *Gonytrichum* sp. Tetrahedron 68(31):6218–6223. https://doi.org/10.1016/j.tet.2012.05.064
6. Ehrlich KC, Lee L, Ciegler A, Palmgren M (1982) Secalonic acid D: natural contaminant of corn dust. Appl Environ Microbiol 44(4):1007–1008. https://doi.org/10.1128/aem.44.4.1007-1008.1982
7. Tuong TL, Aree T, Do LTM, Nguyen PKP, Wongana P, Chavasiri W (2019) Dimeric tetrahydroxanthones from the lichen *Usnea aciculifera*. Fitoterapia 137:104194. https://doi.org/10.1016/j.fitote.2019.104194
8. Nguyen V-K, Nguyen-Si H-V, Devi AP, Poonsukkho P, Sangvichien E, Tran T-N, Yusuke H, Mitsunaga T, Chavasiri W (2021) Eumitrins FH: three new xanthone dimers from the lichen *Usnea baileyi* and their biological activities. Nat Prod Res. https://doi.org/10.1080/14786419.2021.2023143
9. Tuong TL, Do LT, Aree T, Wonganan P, Chavasiri W (2020) Tetrahydroxanthone–chromanone heterodimers from lichen *Usnea aciculifera* and their cytotoxic activity against human cancer cell lines. Fitoterapia 147:104732. https://doi.org/10.1016/j.fitote.2020.104732
10. Wu G, Yu G, Kurtan T, Mandi A, Peng J, Mo X, Liu M, Li H, Sun X, Li J (2015) Versixanthones A-F, cytotoxic xanthone–chromanone dimers from the marine-derived fungus *Aspergillus versicolor* HDN1009. J Nat Prod 78(11):2691–2698. https://doi.org/10.1021/acs.jnatprod.5b00636
11. Yang D-M, Takeda N, Iitaka Y, Sankawa V, Shibata S (1973) The structures of eumitrins A1, A2 and B. Tetrahedron 29(3):519–528. https://doi.org/10.1016/0040-4020(73)80003-1
12. Nguyen V-K, Genta-Jouve G, Duong T-H, Beniddir MA, Gallard J-F, Ferron S, Boustie J, Mouray E, Grellier P, Chavasiri W (2020) Eumitrins CE: Structurally diverse xanthone dimers from the vietnamese lichen *Usnea baileyi*. Fitoterapia 141:104449. https://doi.org/10.1016/j.fitote.2019.104449
13. Li T-X, Yang M-H, Wang Y, Wang X-B, Luo J, Luo J-G, Kong L-Y (2016) Unusual dimeric tetrahydroxanthone derivatives from *Aspergillus lentulus* and the determination of their axial chiralities. Sci Rep 6:38958. https://doi.org/10.1038/srep38958
14. Nguyen V-K, Duong T-H, Nguyen KPP, Sangvichien E, Wonganan P, Chavasiri W (2018) Chemical constituents of the lichen *Usnea baileyi* (Stirt.) Zahlbr. Tetrahedron Lett 59(14):1348–1351. https://doi.org/10.1016/j.tetlet.2018.02.007
15. Din LB, Zakaria Z, Samsudin MW, Elix JA (2010) Chemical profile of compounds from Lichens of Bukit Larut, Peninsular Malaysia. Sains Malays 39(6):901–908
16. Giralt M (2010) New morphological and chemical data for *Buellia imshaugii*. Lichenologist 42(6):763–765. https://doi.org/10.1017/S0024282910000472

17. Bungartz F, Elix JA, Nash TH III (2004) The genus *Buellia sensu lato* in the Greater Sonoran Desert Region: saxicolous species with one-septate ascospores containing xanthones. Bryologist 107(4):459–547. https://doi.org/10.1639/0007-2745(2004)107[459:TGBSLI]2.0.CO;2
18. Lendemer JC, Sheard JW, Göran T, Tønsberg T (2012) *Rinodina chrysidia*ta, a new species from far eastern Asia and the Appalachian Mountains of North America. Lichenologist 44(2):179–187. https://doi.org/10.1017/S0024282911000764
19. Zhang W, Krohn K, Flörke U, Pescitelli G, Di Bari L, Antus S, Kurtán T, Rheinheimer J, Draeger S, Schulz B (2008) New mono-and dimeric members of the secalonic acid family: blennolides A-G isolated from the fungus *Blennoria* sp. Chem Eur J 14(16):4913–4923. https://doi.org/10.1002/chem.200800035
20. El-Elimat T, Figueroa M, Raja HA, Graf T, Swanson SM, Falkinham JO III, Wani MC, Pearce CJ, Oberlies NH (2015) Biosynthetically distinct cytotoxic polyketides from *Setophoma terrestris*. Eur J Org Chem 2015(1):109–121. https://doi.org/10.1002/ejoc.201402984
21. Grimme S (2019) Exploration of chemical compound, conformer, and reaction space with meta-dynamics simulations based on tight-binding quantum chemical calculations. J Chem Theory Comput 15(5):2847–2862. https://doi.org/10.1021/acs.jctc.9b00143
22. Pracht P, Bohle F, Grimme S (2020) Automated exploration of the low-energy chemical space with fast quantum chemical methods. Phys Chem Chem Phys 22(14):7169–7192. https://doi.org/10.1039/C9CP06869D
23. Neese F, Wennmohs F, Becker U, Riplinger C (2020) The ORCA quantum chemistry program package. J Chem Phys 152(22):224108. https://doi.org/10.1063/5.0004608
24. Smith SG, Goodman JM (2010) Assigning stereochemistry to single diastereoisomers by GIAO NMR calculation: the DP4 probability. J Am Chem Soc 132(37):12946–12959. https://doi.org/10.1021/ja105035r
25. Grimblat N, Gavín JA, Hernández Daranas A, Sarotti AM (2019) Combining the power of J coupling and DP4 analysis on stereochemical assignments: the J-DP4 methods. Org Lett 21(11):4003–4007. https://doi.org/10.1021/acs.orglett.9b01193

Authors and Affiliations

Van-Kieu Nguyen[1,2] · Phan-Si-Nguyen Dong[1,2] · Hoai-Vu Nguyen-Si[1,2] · Ek Sangvichien[3] · Thanh-Nha Tran[4] · Le-Thuy-Thuy-Trang Hoang[4] · Minh-Trung Dao[4] · Hai-Nguyen[1,2] · Hoang-Vinh-Truong Phan[1,2] · Hioki Yusuke[5] · Tohru Mitsunaga[6] · Warinthorn Chavasiri[7]

✉ Van-Kieu Nguyen
nguyenvankieu2@duytan.edu.vn

✉ Warinthorn Chavasiri
warinthorn.c@chula.ac.th

1 Institute of Fundamental and Applied Sciences, Duy Tan University, Ho Chi Minh City, Vietnam

2 Faculty of Natural Sciences, Duy Tan University, Da Nang, Vietnam

3 Lichen Research Unit and Lichen Herbarium, Department of Biology, Faculty of Science, Ramkhamhaeng University, Bangkapi, Bangkok 10240, Thailand

4 Department of Environmental Engineering, Thu Dau Mot University, Binh Duong, Vietnam

5 Graduate School of Natural Science and Technology, Gifu University, 1-1 Yanagido, Gifu 501-1193, Japan

6 Faculty of Applied Biological Sciences, Gifu University, 1-1 Yanagido, Gifu 501-1193, Japan

7 Center of Excellence in Natural Products Chemistry, Department of Chemistry, Faculty of Science, Chulalongkorn University, Pathumwan, Bangkok 10330, Thailand